

A note on the existence of a low-level southerly jet along the Benguela coast
of Southern Africa

Sharon E. Nicholson
Department of Meteorology
Florida State University
Tallahassee FL 32306
sen@met.fsu.edu

Submitted to
The Journal of Climate
January, 2008

ABSTRACT

A major focus of global climate change is the role of Atlantic Ocean in climate variability. In this article, evidence is presented of the existence of a low-level jet stream along the Benguela coast of the Atlantic that may play a major role in transmitting the Atlantic's influence to many regions of Africa. Here this feature, termed the Benguela Jet, is described for the first time. Its climatology and kinematic signature are examined and its possible links to ENSO and coastal rainfall variability are evaluated.

1. Introduction

Coastal jets have been shown to play an important role in climate in several parts of the world. The most notable example is the Somali or Findlater Jet that extends across the western Indian Ocean from East Africa to India (Findlater 1969). This jet is an important component of the Indian monsoon system and plays a role in intraseasonal and interannual variability (e.g., Webster and Hoyos 2004). Another notable example is the Peruvian jet in the eastern Pacific along the desert coastal strip (Lettau 1978). This jet enhances coastal upwelling and aridity, creating the world's most arid climate. Its northern-hemisphere analog is a north-northwesterly jet off the coast of southern California (Parish 2000). Further south, a low-level jet in the Gulf of California, has been shown to provide important moisture pulses linked to the North American monsoon (Douglas 1995).

The three jets described above have several geographical commonalities, in addition to their coastal locations. Each is associated with a longshore, cold current. Each extends along a thermal gradient between cold, upwelled water and coastal mountain ranges. Each is a low-level wind maximum that parallels a coastal desert. This is precisely the situation that exists along the Benguela Coast of the southeastern Atlantic. A strong temperature gradient is imposed by the juxtaposition of the cold Benguela current and the highland regions of Namibia, as well as the Angolan highlands. A hyper-arid desert strip, with aridity rivaling that of the Peruvian desert, extends from 15 ° S to 30 ° S (Fig. 1).

The presence of these geographical factors suggests the possible existence of a low-level jet along the Benguela coast of Africa. In this article such a feature, henceforth termed the Benguela Jet, is documented for the first time. The analysis is based on wind data from NCEP Reanalysis (Kalnay et al. 1996). The jet's links to sea-surface temperatures along the Benguela

coast are demonstrated. The relationship between this jet and the interannual variability of rainfall and its potential role in transmitting the effects of Atlantic variability to the rainfall regime over Africa are also discussed.

2. Mean winds along the Benguela coast

Fig. 2 shows the annual mean vector winds at 1000 hPa. A jet-like wind maximum is evident from 20 ° to 25 ° S at 10 ° E, some 300 km off the coast of Namibia. It lies on the northeastern flank of the Ste. Helen (South Atlantic) High, which is evident from the anticyclonic pattern of winds. Within this area the winds are almost uniformly southeasterly, so that the jet parallels the Namib coast. Annual mean wind speeds exceed 8 ms⁻¹ in the core of the jet. Thus its intensity exceeds that of the Peruvian Jet, with mean core speeds on the order of 6 ms⁻¹. To the north and east of the jet core the winds take on a more easterly component, but remain moderately strong (in excess of 6 ms⁻¹). This area of strong winds covers the entire region of the Benguela current, into the mid-Atlantic.

Fig. 3 depicts the mean vector winds from January to December. Strong seasonal variations are apparent in both the intensity and location of the Benguela Jet. During the jet's seasonal excursion, its latitude roughly parallels the seasonal displacements of the high. The jet's core reaches its southern-most latitude, 26 ° S, in January and its northern-most in May, when it lies at 15 ° S. Thus, its seasonal displacement is roughly 11 degrees of latitude.

The jet is strongest in October, when its mean speed exceeds 10 m s⁻¹ in the core. In this month, it extends from 15 ° S to 32 °S and maximum winds are roughly 6 degrees of longitude (650 km) off-shore. The jet is weakest in May and June, when the core speed is roughly 8.5 ms⁻¹. It is evident throughout the year at 1000 hPa, but it disappears at 925 hPa from April to August. From October to December it is nearly as strong at 925 hPa (10 ms⁻¹) as at 1000 hPa.

3. Sea-surface temperatures along the Benguela coast

Along cold-water coasts a strong feedback relationship exists between the ocean and the atmosphere. The high wind speeds on the eastern flank of the high produce the upwelling of cold-water, which in turn intensifies wind speeds near the region of upwelling by way of the thermal wind relationship (Lettau 1978). Thus, a close relationship between sea-level pressure, the intensity of the jet, and sea-surface temperatures would be anticipated.

Figure 4 shows the annual mean sea-surface temperatures (SSTs) in the southeastern Atlantic and surface current vectors. SSTs are taken from the NOAA Extended Reconstructed Sea Surface Temperature data set (Smith and Reynolds, 2004). The cold region of coastal upwelling is evidenced by temperatures on the order of 15 to 18 ° C. Water flows in a northerly to northwesterly direction. It flows more or less parallel to the shore, but with a small offshore component. This off-shore component is co-located with the region of coldest temperatures/strongest upwelling, situated within roughly 200 to 300 km of the shore and extending from 20 ° to 35 ° S. The maximum surface wind speeds are also coincident with the region of lowest temperatures.

Figure 5 shows the monthly mean SSTs for the core of the upwelling region, based on the Smith/Reynolds data set. The variations in SST largely reflect the intensity of upwelling, but the annual cycle also has an influence. Temperatures range from 17.6 ° C in February to 14.1 ° C in July and August. An analysis by Höflich (1984), based on data from the Deutsche Seewarte in Hamburg, indicates even colder temperatures. Coastal water temperatures in July are below 12 ° C from roughly 20 ° S to 33 ° S.

The monthly mean pressure gradient at the latitude of the jet core and the speed of the jet core are also indicated in Fig. 5. A comparison of the three variables shows a strong but

complex relationship among them. When upwelling is most intense/SSTs lowest, in late winter or spring, the surface pressure gradient is large and the Benguela jet is strong. In contrast, the pressure gradient, speed of the jet and SSTs show parallel trends during the warmer months from December to May. All three variables decrease rapidly between January and May. This probably reflects the annual cycle, while the relationship among the variables later in the year reflects the feedback among the wind, pressure and SSTs.

For the most part, the strength of the jet parallels the large-scale pressure gradient, suggesting geostrophic balance. However, the sharp decrease in the core speed of the jet from October to November is not commensurate with a decrease in the large reduction of the surface pressure gradient. Coastal SSTs do increase abruptly from October to November, probably reflecting the seasonal warming as the boreal summer sets in. Presumably, the SSTs during these months locally modify the pressure gradient, reducing the strength of the low-level jet, although the large-scale pressure gradient remains strong.

4. Low-level circulation

Figure 6 presents the vertical cross-section of the wind in the Benguela Jet during October. The southerly jet is apparent at levels below 925 hPa. Its core is elevated and the maximum speed is at 1000 hPa. This is the case in all other months, as well.

Figure 7 presents mean wind divergence for October at the surface and at 1000 hPa. Fig. 8 shows mean sea-surface temperature in October. Collectively these variables suggest that upwelling is evident not only along the coast, but in the south-central Atlantic. The control of coastal upwelling by the surface wind is demonstrated by the divergence pattern. Strong divergence (up to $11 \times 10^{-6} \text{ s}^{-1}$) parallels the coast, consistent with the coastal aridity. Maximum divergence is at the surface in the region of the Benguela Jet, but a strong core of divergent flow

coincident with the jet is evident also at 1000 hPa and even 925 hPa (not shown). Divergence is also apparent in association with the second wind maximum in the south-central Atlantic.

The SSTs indicate a cold tongue penetrating well into the central Atlantic and extending to near the equator. While advection of cold water from higher latitudes can explain much of the SST pattern, the divergent flow suggests a contribution from upwelling as well.

Fig. 9 shows the vertical motion at both 1000 hPa and 925 hPa. At 1000 hPa there is a small area of strong subsidence, with omega reaching .02 to .03 Pa s⁻¹. Much more prominent is a region of strong ascent that stretches along the coast from 5 ° S to 35 ° S. Its seaward extent coincides with the core of the jet. The ascent, which exceeds 0.08 Pa s⁻¹ over a large region, is probably associated with the local sea-breeze circulation.

Just above the jet maximum, at 925 hPa, there is a large region of subsidence coincident with the core of the jet. Omega reaches 6 Pa s⁻¹. The area of ascent is significantly weaker than at 925 hPa and generally confined to land areas. Overall, this circulation is reminiscent of the helical circulation around the Peruvian jet, as described by Lettau (1978). It should be noted, however, that 925 hPa is below much of the coastal land mass. Although NCEP Reanalysis "corrects" for the situation, the analysis over land must be interpreted cautiously.

5. Interannual variability and links to El Niño

An El Nino-like phenomenon occurs along the Benguela Coast, with marked warming in some years (Covey and Hastenrath 1978, Walker et al. 1984, Rouault et al. 2003). This warming, termed the Benguela Niño, is associated with tremendous amounts of precipitation along the coast, similar to what occurs along the Peruvian coast during el Niño. This phenomenon is most pronounced in March and April (Shannon et al. 1986, Nicholson and Entekhabi 1987, Nicholson and Kim 1997, Florenchie et al. 2004, Gu and Adler 2006), when the Benguela Jet is

normally weakest and its aridifying influence is minimized. Northern sectors of the Benguela coast receive 20 to 50 mm during these March and April in cold-water years but some 100 to 400 mm mo⁻¹ during warm events. The warming is most pronounced at the northern edge of the jet core, in the region of confluence between the Angolan and Benguela currents. These facts suggest a possible link between the jet and the interannual variability of rainfall.

Further interesting is that the warm events bear some relationship to the Pacific el Niño (Gillooly and Walker 1984, Shannon et al. 1986, Nicholson and Entekhabi 1987, Reason 2000), with warming in the southeastern Atlantic beginning abruptly around January of the el Niño year and persisting throughout that year (Nicholson 1997). The warming gets markedly stronger in April of that year. Cooling generally begins in January of the post-el Niño year and reaches a maximum around April of that year. There also appears to be a link between the Benguela Niños and the Atlantic Niño (Gu and Adler 2006).

To examine the relationships among rainfall variability, the Benguela Jet and el Niño, a two-part analysis was carried out. First, a preliminary analysis examined SSTs in April and wind speeds in January, as these are the months in which a link to el Niño is most likely to be evident (Nicholson 2008). To permit a comparison between the jet and rainfall variability, seasonal data were also analyzed. SSTs were evaluated at 17 ° S, i.e., at the northern edge of the Benguela Jet and near the confluence of the Benguela and Angola currents. Winds speeds were evaluated near the core of the Benguela Jet.. These were calculated by finding the maximum wind speed at 1000 hPa within the box shown in Fig. 7. The el Niño years are based on warm episodes identified by the NOAA Climate Prediction Center, using the Oceanic Niño Index (ONI) based on SSTs in the Niño 3.4 region of the Pacific. The 1953 episode, identified and utilized in earlier studies, was added to our analysis.

Figure 10 shows the time series of April SSTs and January wind speeds. In Fig. 10a el Niño years are shaded; in Fig. 10b post-el Niño years are shaded. During most of the el Niños positive SST anomalies appear in April, but strong negative anomalies are also apparent in some el Niño years. In most of cases the negative anomalies appeared in the second year of a two-year el Niño event. Positive anomalies did not mark the 1957 episode, but SSTs were markedly higher that year than in the previous and subsequent years. In contrast to SSTs, January wind speeds in the core of the Benguela Jet do not show any consistent change during el Niño years. In the post-el Niño year, a much more consistent signal is apparent in both SSTs and wind (Fig. 10b). During most episodes a wind speed maximum appears in January of the post-el Niño year and an SST minimum appears the following April. Overall these preliminary results indicate that some relationship exists between the Benguela Jet and coastal temperatures, but that it is stronger during the post-el Niño cooling.

To further examine this conclusion and to directly compare rainfall and wind anomalies, the analysis was extended to cover the entire year. Figs. 11 and 12 show seasonal mean temperature anomalies from 1948 to 2005 at 17 ° S, the same latitude shown in Fig. 10. These are expressed as a departure from a seasonal mean, calculated for the years 1948 to 2005. In Fig. 11 el Niño years are shaded and in Fig. 12 post-el Niño years are shaded.

Wind anomalies corresponding to the core of the Benguela jet are also indicated in both figures. These were calculated as in Fig. 10. However, the wind speed was expressed as a departure from a monthly mean core speed and three-month averages were calculated. The result showed significant multi-decadal scale variability, upon which lower-frequency interannual components are superimposed. Low-frequency modes, such as the Atlantic Multi-decadal Oscillation (AMO) or the Inter-hemispheric Mode, are well-known in the Atlantic (Carton et al. 1996, Mehta 1998, Enfield and Mestas-Nuñez 1999, Ruiz-Baradas et al. 2000,

Marshall et al.). The interannual components are largely forced by ENSO (Czaja et al. 2002). To isolate these higher frequency components, a ten-year running mean is shown in the wind plots and shading indicates departures from the ten-year running mean.

Figure 11 confirms that warmings do appear along the Benguela coast during most el Niño years, but it is often short-lived. During most episodes there is an abrupt warming and strong positive anomalies are evident during the el Niño year. However, during many episodes strong negative anomalies are evident within the same year. The association between warmings and el Niño is strongest prior to late 1970s, at which time a major change occurred in the amplitude, period, spatial structure and temporal evolution of el Niño (An and Jin 2000, An and Wang 2000). It is interesting to note, however, that a fairly good correspondence exists between weakening of the jet and abrupt warming. Also, the weakening of the jet occurs rather consistently during el Niño episodes. This may be related to a weakening of the Angolan low that occurs during most el Niño episodes (Reason et al. 2006).

Again a much more consistent signal is evident in the post-el Niño year (Fig. 12). During most el Niños, strong negative anomalies appear, consistent with the results shown in Fig. 10b. The appearance of the cold anomalies generally coincides with accelerations of the Benguela Jet.

These results suggest that the link to el Niño is stronger for the post-el Niño cold episodes in the Atlantic than for the warm episodes. This is consistent with the idea that a strong feedback exists between the speed of the Benguela Jet and coastal SSTs. Although the core is at 1000 hPa the jet is strong at the surface as well. An intensification of the jet would intensify upwelling and reducing SSTs. On the other hand, the warming tends to occur during the months of March to May (Florenchie et al. 2004), when both the jet and coastal upwelling are

relatively weak. Further weakening of the jet would probably not greatly influence SSTs. This may be the reason for the weaker association between the warmings and el Niño.

Another possible explanation for the weaker association with coastal warming is the phenomenon termed Atlantic Niño II by Okumura and Xie (2006). These are warm episodes in the equatorial Atlantic that occur in October and November, when the Benguela Jet is particularly strong and SST variability along the coast is particularly weak (Gu and Adler 2006). High rainfall occurs along the Benguela Coast during these warmings, the occurrence of which is completely uncorrelated with el Niño.

6. Summary and Conclusions

A low-level jet with a core at approximately 1,000 hPa parallels the Benguela coast of Southern Africa, in the southeastern Atlantic. Maximum winds are roughly 650 km off-shore. Strong seasonal variations are apparent in both its intensity and location. Peak intensity is reached in October, when the monthly mean wind speed of its core exceeds 10 ms^{-1} . The jet is weakest in May and June, but the core speed is still 8 to 9 ms^{-1} , on average. The jet coincides with the hyperarid Namib coastal desert. At the jet's northern extreme around 15° S , where winds take on an easterly component, the rainfall gradient is intense and the shift from extreme aridity to semi-arid conditions is abrupt. The coincidence suggests that it plays some role in producing the hyperarid conditions of the Namib.

The Benguela jet lies on the northeastern flank of the Ste. Helen (South Atlantic) High. The high is evident from the vector winds in Fig. 2. During the jet's seasonal excursion, its latitude roughly parallels the seasonal displacements of the high. The core of the Benguela Jet reaches its southern-most latitude, 26° S , in January, and its northern-most in May, when it lies at 15° S . Thus, its seasonal displacement is roughly 11 degrees of latitude.

The jet tends to weaken during el Niño years and strengthen during the following year. This is consistent with the pressure analysis of Nicholson (1997), showing a weakening of the Ste. Helena high during the el Niño years and an intensification of the high in the post-el Niño year. The intensification is pronounced early in that year, accounting for the intensification of the jet in January of the post-el Niño year, as noted earlier. The timing of the weakening of the high in the el Niño year is more variable, so that the weakening of the jet is apparent in the annual analysis (Fig. 11), but not in the analysis limited to January (Fig. 10).

A relationship between the strength of the Benguela Jet and coastal SSTs is also apparent, with a stronger/weaker jet corresponding to lower/higher SSTs. This is indicative of the feedback between these two variables and the association is strongest during the months when the jet is generally weak (March to May). When the jet becomes anomalously strong, upwelling increases and coastal temperatures are reduced. A weaker relationship is evident between weakening of the jet and coastal warming. However, the intensity of the warming and the extreme variability of coastal rainfall during March and April suggest that the jet does play some role in enhancing the warming. A similar low-level jet may play a role in enhancing variability in the equatorial Atlantic (Grotsky et al. 2003).

A very open question is the extent to which the Benguela Jet might have an impact on variability elsewhere over Africa. SST variability along the Benguela Coast of the southeastern Atlantic is strongly linked to rainfall variability in western equatorial Africa (Balas et al. 2007) and East Africa (Nicholson and Entekhabi 1987). Several authors have suggested that SSTs in the South Atlantic also impact Sahel rainfall (Camberlin et al. 2001, Trzaska et al. 1996). The Benguela Jet may be one link in these relationships and its importance may extend well beyond the Benguela coast.

Acknowledgements

The author would like to thank computer programmer, Mr. Douglas Klotter, for his assistance in the production of figures. This work was supported by a Climate Dynamics grant from the National Science Foundation, ATM-0004479.

References

An, S.-I., and F.-F. Jin, 2000: An eigen analysis of the interdecadal changes in the structure and frequency of ENSO mode. *Geophys. Res. Lett.*, **27**, 2573-2576.

An, S. I., and B. Wang, 2000: Interdecadal change of the structure of the ENSO mode and its impact on the ENSO frequency. *J. Climate*, **13**, 2044-2055.

Balas, N., S. E. Nicholson, and D. Klotter, 2007: The relationship of rainfall variability in West central Africa to sea-surface temperature fluctuations. *Int. J. Climatol.*, **27**, 1335-1349.

Camberlin, P., S. J. Anicot, and I. Pocard, 2001: Seasonality and atmospheric dynamics of the teleconnection between African rainfall and tropical sea-surface temperature: Atlantic vs. ENSO. *Int. J. Climatol.*, **21**, 973-1005.

Carton, J. A., X. Cao, B. S. Giese, and A. M. da Silva, 1996: Decadal and interannual SST variability in the tropical Atlantic. *J. Phys. Oceanogr.*, **26**, 1165-1175.

Covey, D. L., and S. Hastenrath, 1978: The Pacific El Niño phenomenon and the Atlantic circulation. *Mon. Wea. Rev.*, **106**, 1280-1286.

Czaja, A., P. van der Vaart, and J. Marshall, 2002: A diagnostic study of the role of remote forcing in tropical Atlantic variability. *J. Climate*, **15**, 3280-3290.

Douglas, M. W., 1995: The summertime low-level jet over the Gulf of California. *Mon. Wea. Rev.*, **123**, 2334-2347.

Enfield, D. B., and A. M. Mestas-Nuñez, 1999: Multiscale variabilities in global sea surface temperatures and their relationship with tropospheric climate patterns. *J. Climate*, **12**, 2719-2733.

Findlater, I., 1969: A major low-level air current near the Indian Ocean during the northern summer. *Quart. J. Roy. Meteor. Soc.*, **95**, 362--380, 1969.

Florenchie, P., C. J. C. Reason, J. R. E. Lutjeharms, and M. Rouault, 2004: Evolution of interannual warm and cold events in the Southeast Atlantic Ocean. *J. Climate*, **17**, 2318-2334.

Gillooly, J. F., and N. D. Walker, 1984: Spatial and temporal behaviour of sea-surface temperatures in the South Atlantic. *S. Afr. J. Sci.*, **80**, 97-100.

Grodsky, S.A., and J. A. Carton, and S. Nigam, 2003: Near surface westerly wind jet in the Atlantic ITCZ. *Geophys. Res. Lett.*, **30** (19), 2009, doi: 10.1029/2003GL017867.

Gu, G., and R. F. Adler, 2006: Interannual rainfall variability in the tropical Atlantic region. *J. Geophys. Res.*, **111**, 2106, doi:10.1029/2005DJ005944.

Höflich, O., 1984: Climate of the South Atlantic Ocean. *World Survey of Climatology*, **15**, H. van Loon, Ed, Elsevier, 1-191.

Kalnay, E., and Coauthors, 1996: The NCEP/NCAR 40-year reanalysis project. *Bull. Amer. Meteor. Soc.*, **77**, 437-471.

Lamb, P. J., and R. A. Pepler, 1992: Further case studies of Tropical Atlantic surface atmospheric and oceanic patterns associated with sub-Saharan drought. *J. Climate*, **5**, 476-488.

Lettau, H. H., 1978: Explaining the World's Driest Climate. *Exploring the World's Driest Climate*, Lettau, H. H., and K. Lettau, Eds. Institute for Environmental Studies, University of Wisconsin, 182-248.

Marshall, J., and Coauthors, 2001: North Atlantic climate variability: Phenomena, impacts, and mechanisms. *Int. J. Climatol.*, **21**, 1863-1898.

Mehta, V. M., 1998: Variability of the tropical ocean surface temperatures at decadal-multidecadal timescales. Part 1: The Atlantic Ocean. *J. Climate*, **11**, 2351-2375.

Nicholson, S. E., 1997: An analysis of the ENSO signal in the tropical Atlantic and western Indian Oceans. *Int. J. Climatol.*, **17**, 345-375.

Nicholson, S. E., 2008: A low-level jet along the Benguela coast, an integral part of the Benguela Current Ecosystem. Submitted to *Climatic Change*.

Nicholson, S. E., and Entekhabi, D., 1987: Rainfall variability in Equatorial and Southern Africa: relationships with sea-surface temperatures along the southwestern coast of Africa. *J. Clim. Appl. Meteor.*, **26**, 561-578.

Nicholson, S.E., and J. Kim, 1997: The relationship of the El Niño-Southern Oscillation to African rainfall. *Int. J. Climatol.*, **17**, 17-135.

Nicholson, S. E., and P. J. Webster, 2008: A physical basis for the interannual variability of rainfall in the Sahel. *Quart. J. Roy. Meteor. Soc.*, in press.

Okumura, Y., and S.-P. Xie, 2006: Some overlooked features of tropical Atlantic climate loading to a new Niño-like phenomenon. *J. Climate*, **19**, 5859-5874.

Parish, T., 2000: Forcing of the summer low-level jet along the California coast. *J. Appl. Meteor.*, **39**, 2421-2433.

Reason, C. J. C., 2000: Multidecadal climate variability in the subtropics/midlatitudes of the Southern Hemisphere oceans. *Tellus*, **52A**, 203-223.

Reason, C. J. C., W. Landman, and W. Tennant, 2006: Seasonal to decadal prediction of Southern African climate and its links with variability of the Atlantic Ocean. *Bull. Amer. Meteor. Soc.*, **87**, 941-955.

Roualt, M., P. Florenchie, N. Fauchereauy, and C. J. C. Reason, 2003: South east Atlantic warm events and southern African rainfall. *Geophys. Res. Lett.*, **30**, 8009, doi:10.1029/2002GL014840.

Ruiz-Barradas, A., J. A. Carton, and S. Nigam, 2000: Structure of interannual-to-decadal climate variability in the tropical Atlantic. *J. Climate*, **13**, 3285-3297.

Shannon, L.V., 1985. The Benguela Ecosystem, I., Evolution of the Benguela, physical features and processes. *Oceanography and Marine Biology*, **23**, 105-182.

Shannon, L.V., A.J. Boyd, G.B. Brundrit and J. Taunton-Clark, 1986: On the existence of an El Niño-type phenomenon in the Benguela system. *J. Mar. Res.*, **44**, 495-520.

Smith, T. M., and R. W. Reynolds, 2004: Improved extended reconstruction of SST (1854-1997). *J. Climate*, **17**, 2466-2477.

Trzaska, S., V. Moron, and B. Fontaine, 1996: Global atmospheric response to specific linear combinations of the main SST modes. Part I: numerical experiments and preliminary results. *Ann. Geophysicae*, **14**, 1066-1077.

Walker, N. D., J. Taunton-Clark, and J. Pugh, 1984: Sea temperatures off the South African west coast as indicators of Benguela warm events. *S. Afr. J. Sci.*, **80**, 72-77.

Webster, P. J, and C. Hoyos, 2004: Prediction of Monsoon Rainfall and River Discharge on 15-30 day Time Scales. *Bull. Amer. Met. Soc.*, **85** (11), 1745-1765.

Figures

1. Rainfall isohyets along the Benguela coast and near-coastal topography. Dashed lines show international borders.

2. Mean vector winds (m s^{-1}) at 1000 hPa, annual average. Contours indicate speed.

3. Monthly mean vector wind speed, January to December (m s^{-1}), at 1000 hPa. Contours indicate speed. Speeds greater than 6 ms^{-1} are shaded.

4. Mean sea-surface temperatures ($^{\circ}\text{C}$) (annual average for the period 1948 to 2005) and surface current in the southeastern Atlantic. SSTs based on data from Smith and Reynolds (2004). Vectors indicate current direction and contours indicate speed (knots/hour) (from Höflich 1984).

5. Monthly SST for the coastal sector of minimum temperatures, surface pressure gradient and maximum speed of the jet core. The pressure gradient is defined as the pressure difference along a 10° longitude sector running centered over the area of maximum winds and perpendicular to the direction of flow.

6. Vertical cross-section of Benguela Jet at 25 ° S as a function of longitude during October.

7. Mean October wind and wind divergence (10^{-6} s^{-1}) at the surface and at 1000 hPa. The indicated box encloses the area in which the jet core can be located during the course of the year.

8. Mean sea-surface temperatures ($^{\circ} \text{C}$) in the southeastern Atlantic (October mean for the period 1948 to 2005).

9. Mean omega (vertical motion, pascals s^{-1}) at 1000 and 925 hPa for October.

10a. April SSTs (17°S , 5°E to 15°E) and January wind speeds in the core of the Benguela jet, at 1000 hPa, 1948 to 2005 (from Nicholson 2008). The core speed of the Benguela Jet is defined as the maximum wind speed at 1000 hPa within the box shown in Fig. 7. El Niño years are shaded.

10b. As in 10 a, but post-el Niño years are shaded.

11. (top) Three-month means of SST anomalies at 17°S (5°E to 15°E), 1948 to 2005 (el Niño years are shaded). (bottom) Core speed of the Benguela Jet, expressed as a three-month departure from the seasonal mean at the location of maximum 1000 hPa winds within the box shown in Fig. 7. Shading expresses departures from a running ten-year mean.

12. (top) Three-month means of SST anomalies at 17° S (5° E to 15° E), 1948 to 2005 (post el Niño years are shaded). (bottom) Core speed of the Benguela Jet, as in Fig. 11.

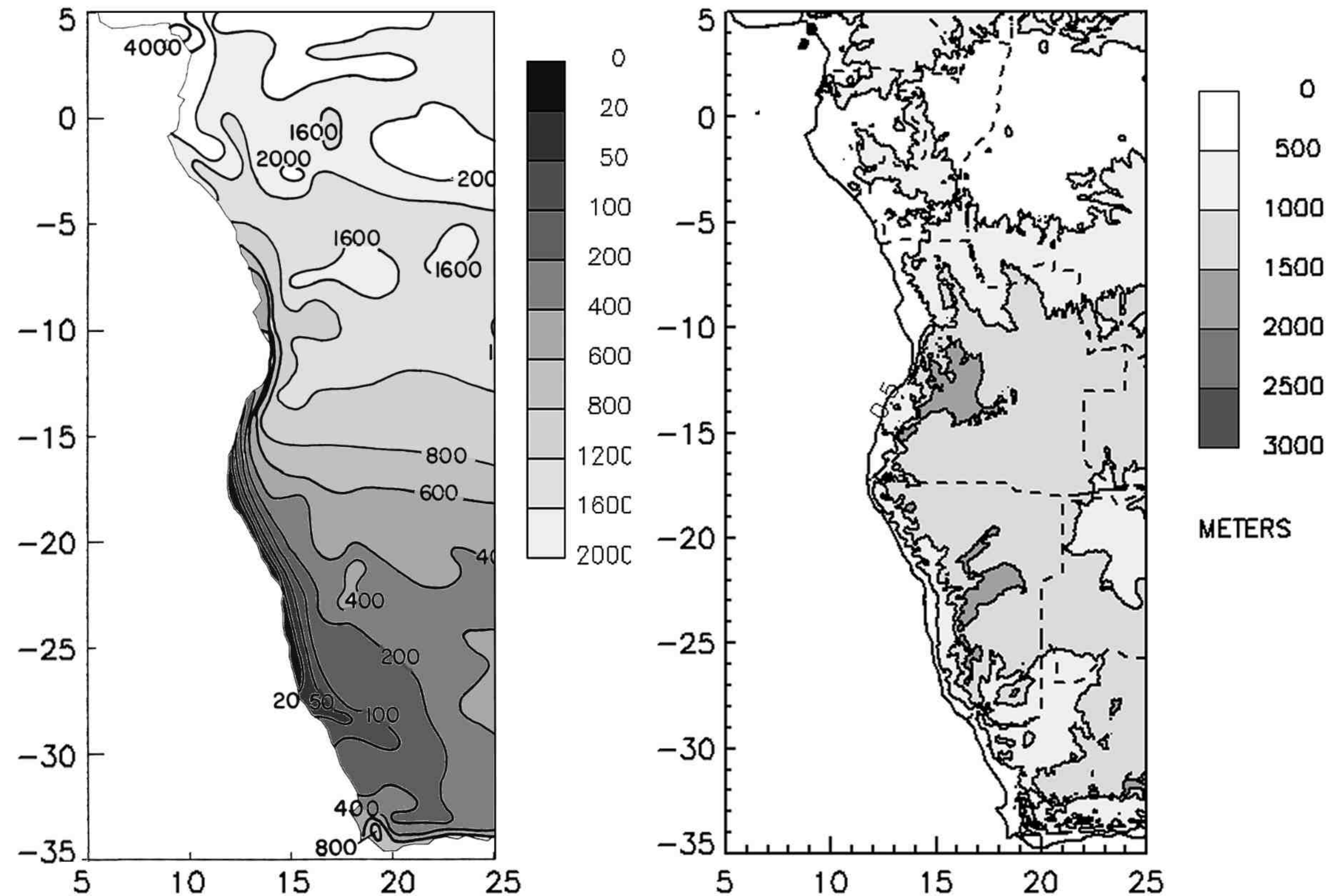


Fig 1. Rainfall isohyets along the Benguela coast and near-coastal topography. Dashed lines show international borders.

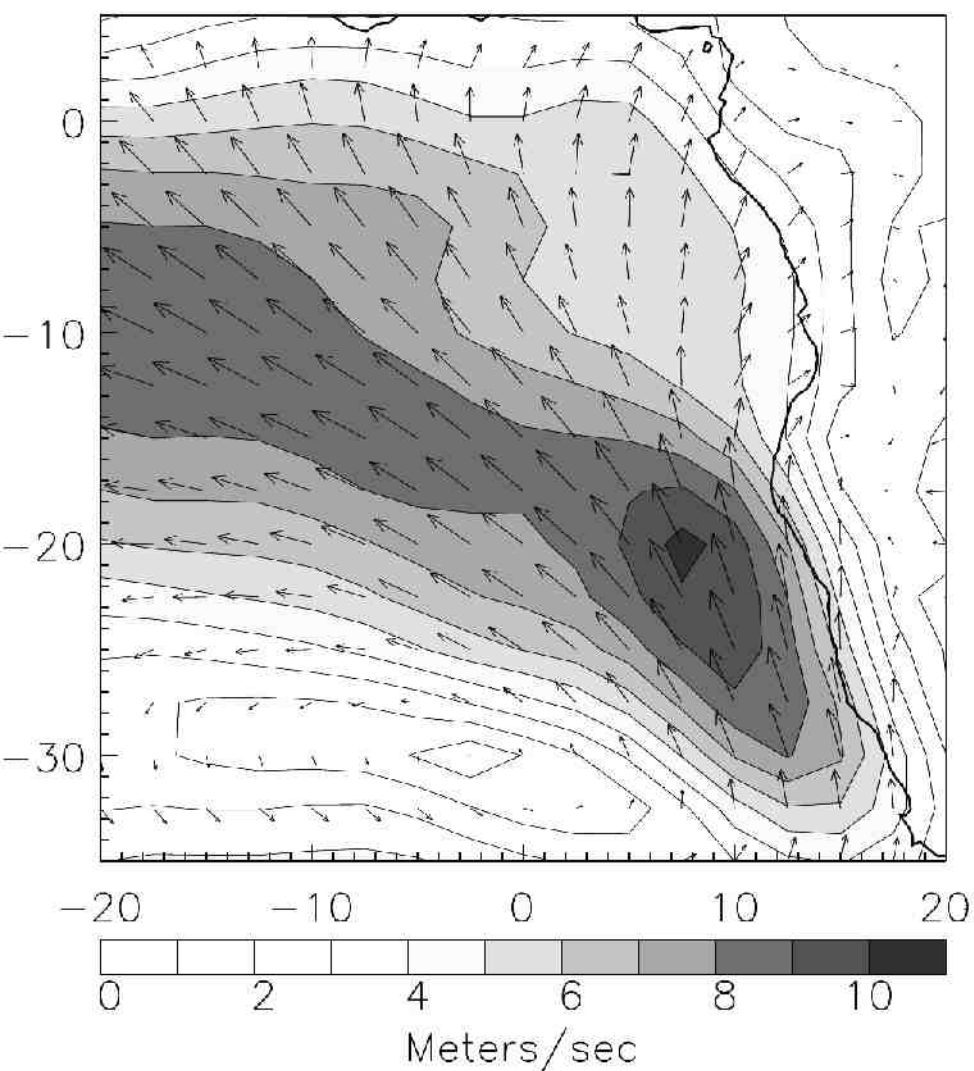


Fig 2. Mean vector winds (m s^{-1}) at 1000 hPa, annual average. Contours indicate speed.

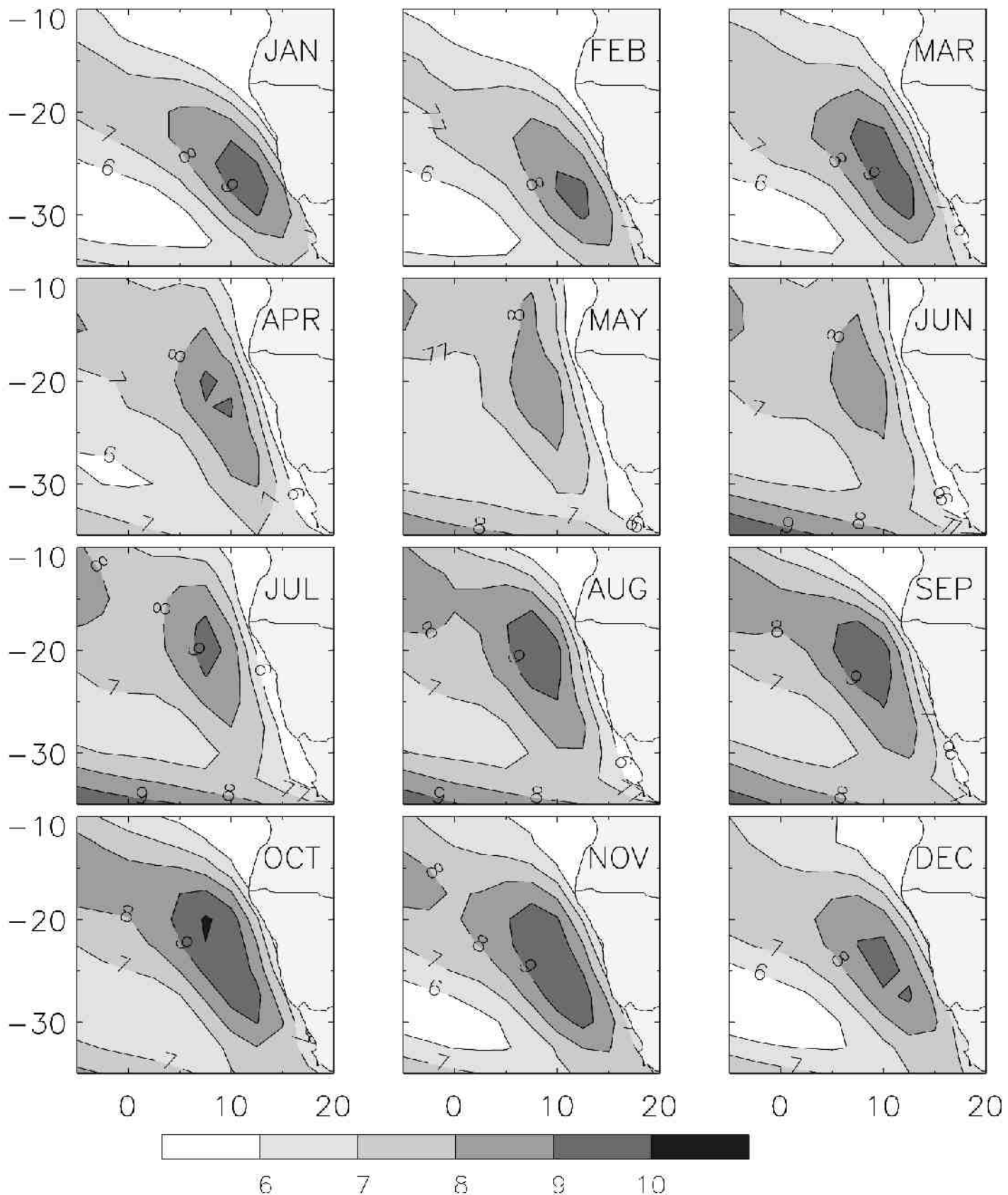


Figure 3. Monthly mean vector wind speed, January to December (m s^{-1}), at 1000 hPa. Contours indicate speed. Speeds greater than 6 m s^{-1} are shaded.

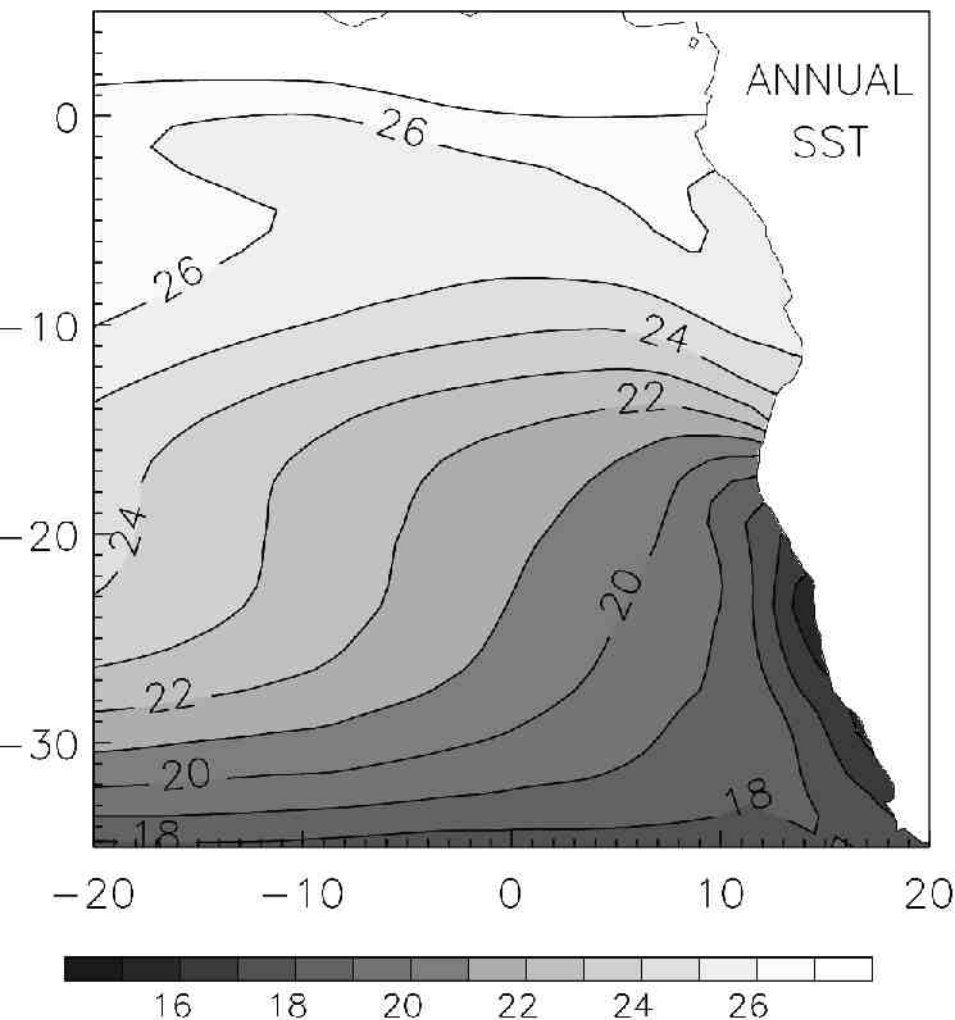


Figure 4A. Mean sea-surface temperatures ($^{\circ}\text{C}$) (annual average for the period 1948 to 2005) and surface current in the southeastern Atlantic. SSTs based on data from Smith and Reynolds (2004). Vectors indicate current direction and contours indicate speed (knots/hour) (from Höflich 1984).

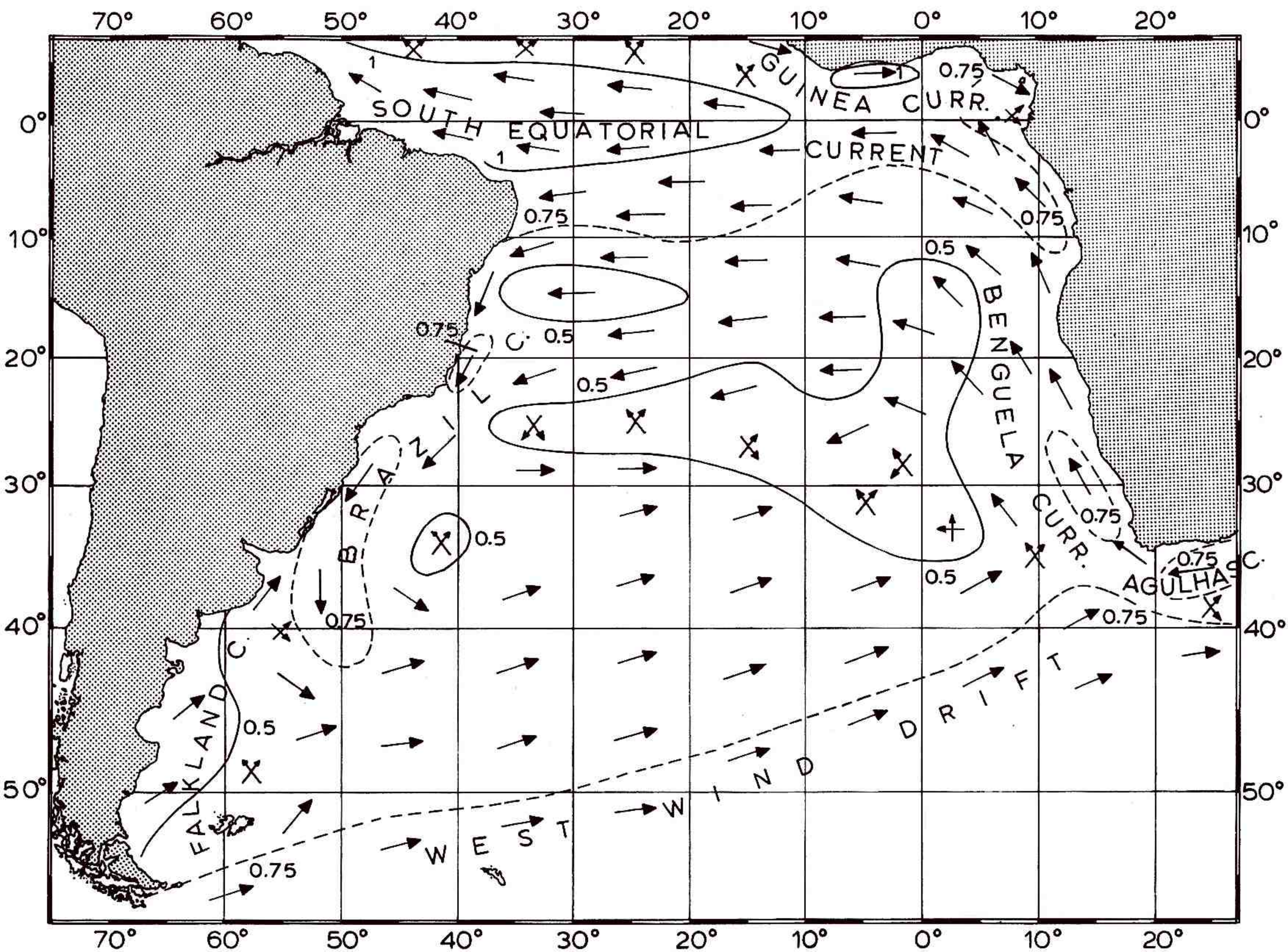


Figure 4B. Mean sea-surface temperatures ($^{\circ}$ C) (annual average for the period 1948 to 2005) and surface current in the southeastern Atlantic. SSTs based on data from Smith and Reynolds (2004). Vectors indicate current direction and contours indicate speed (knots/hour) (from Höflich 1984).

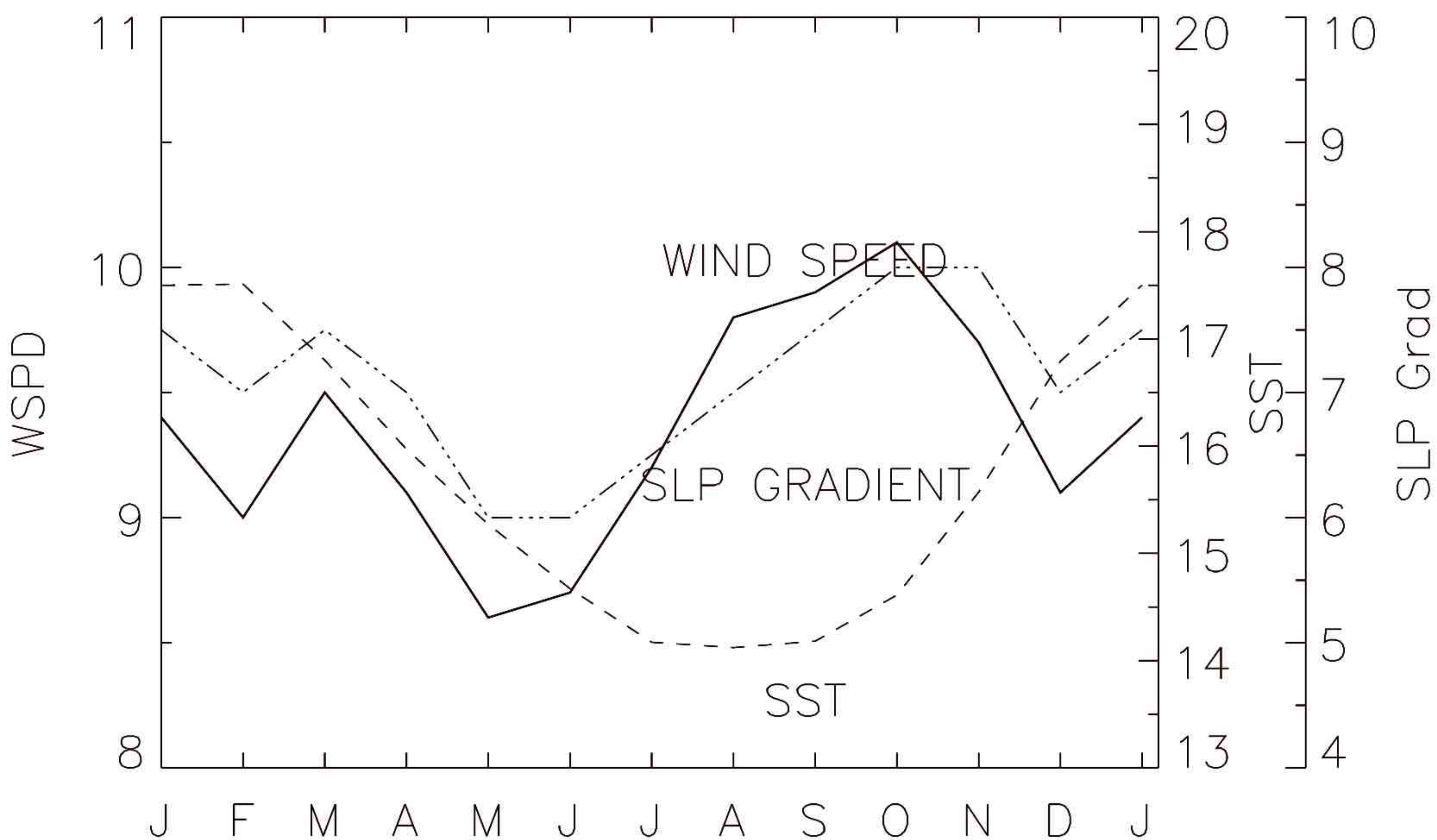


Figure 5. Monthly SST for the coastal sector of minimum temperatures, surface pressure gradient and maximum speed of the jet core. The pressure gradient is defined as the pressure difference along a 10° longitude sector running centered over the area of maximum winds and perpendicular to the direction of flow.

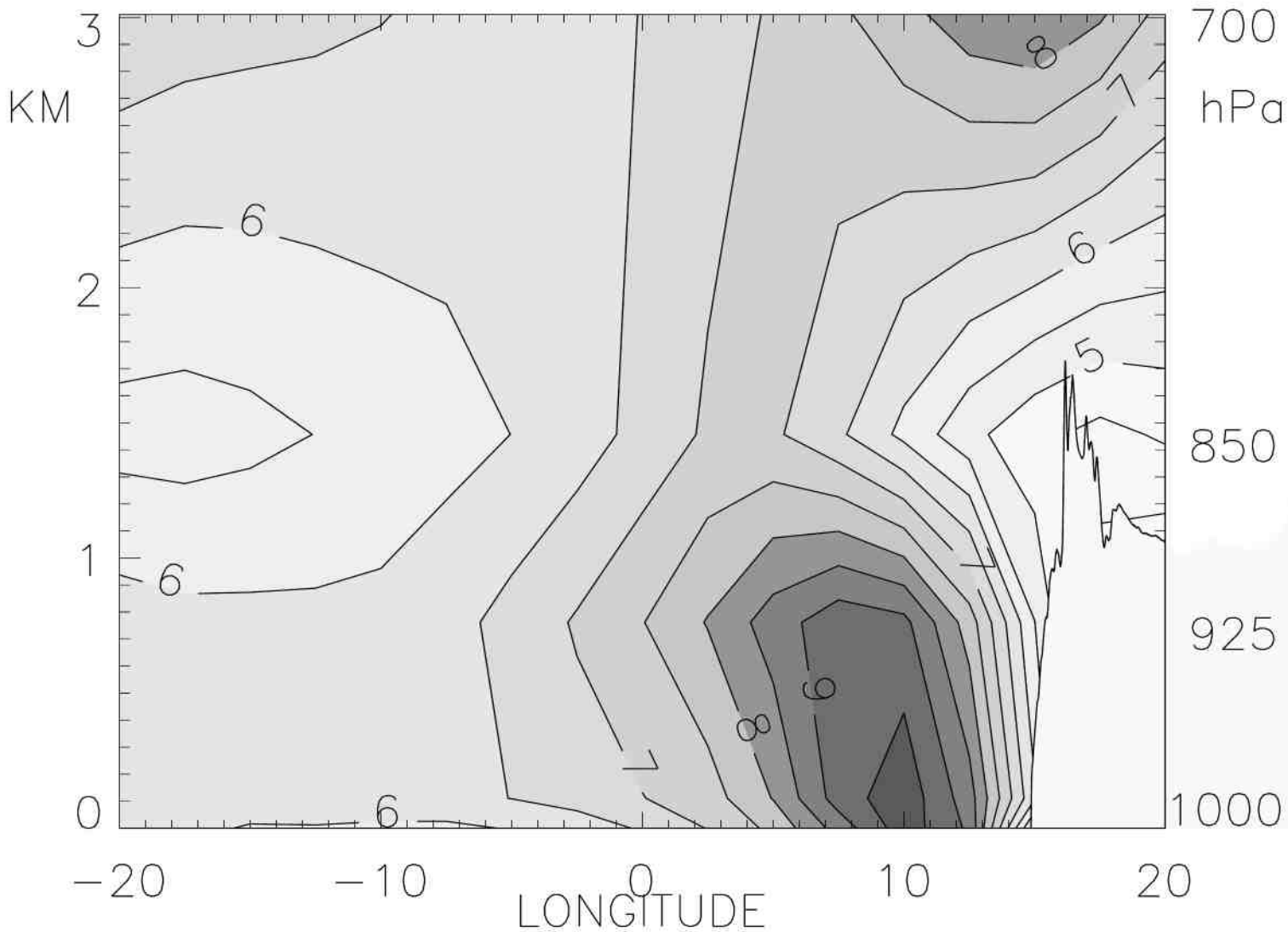
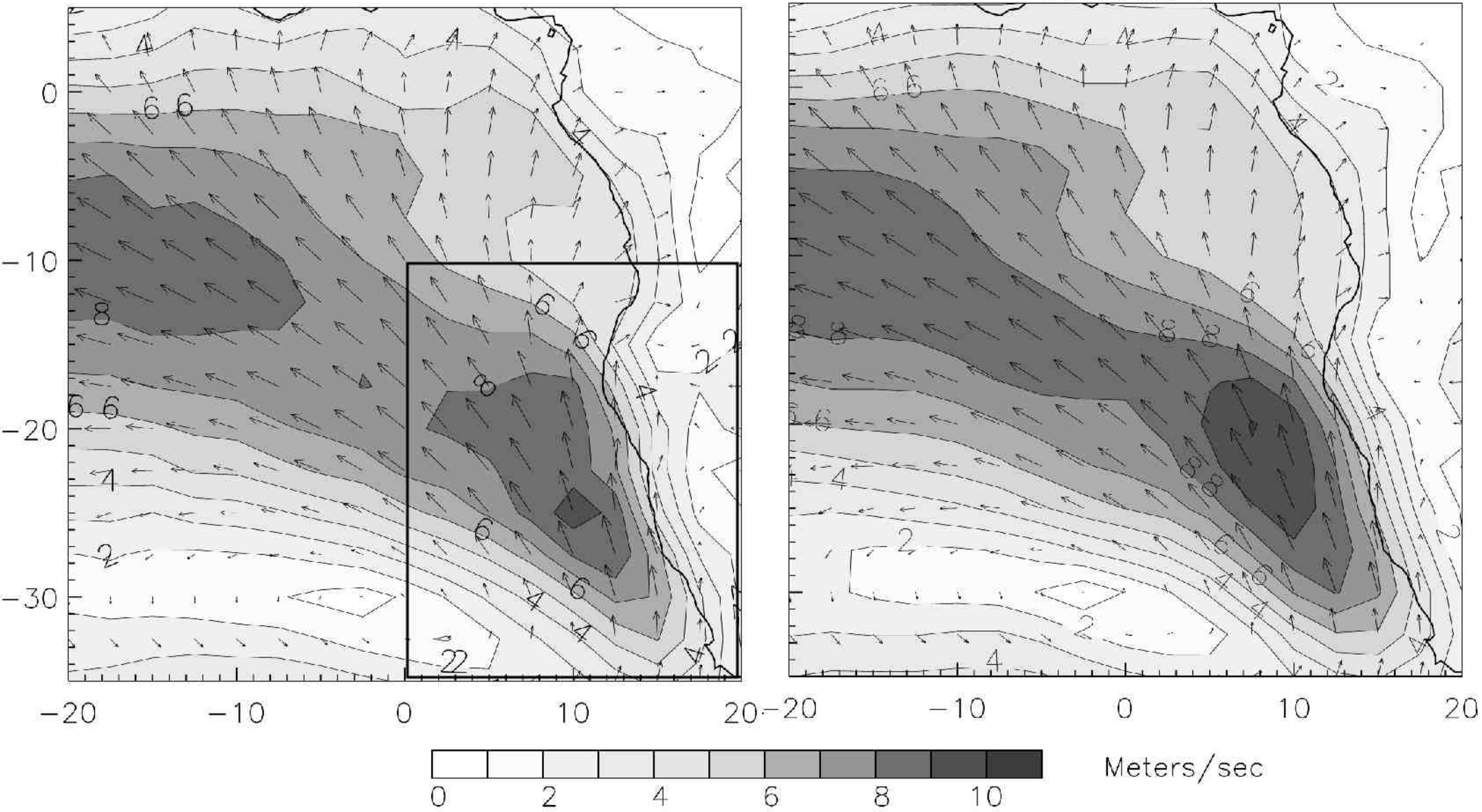


Figure 6. Vertical cross-section of Benguela Jet at 25° S as a function of longitude during October.

WIND SPEEDS AND VECTORS

SURFACE

1000 MB



DIVERGENCE

SURFACE

1000 MB

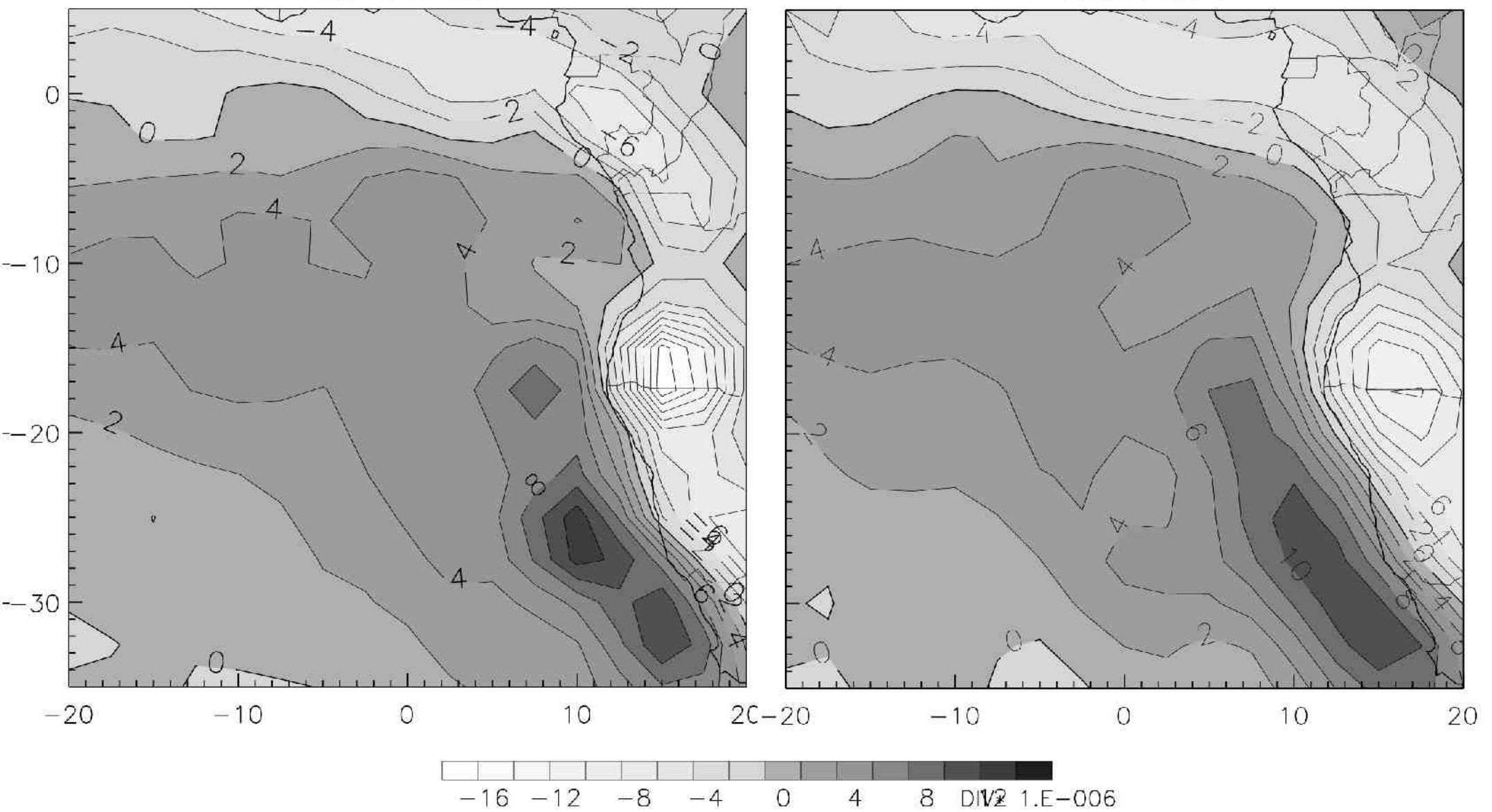


Figure 7. Mean October wind and wind divergence (10^{-6} s^{-1}) at the surface and at 1000 hPa. The indicated box encloses the area in which the jet core can be located during the course of the year.

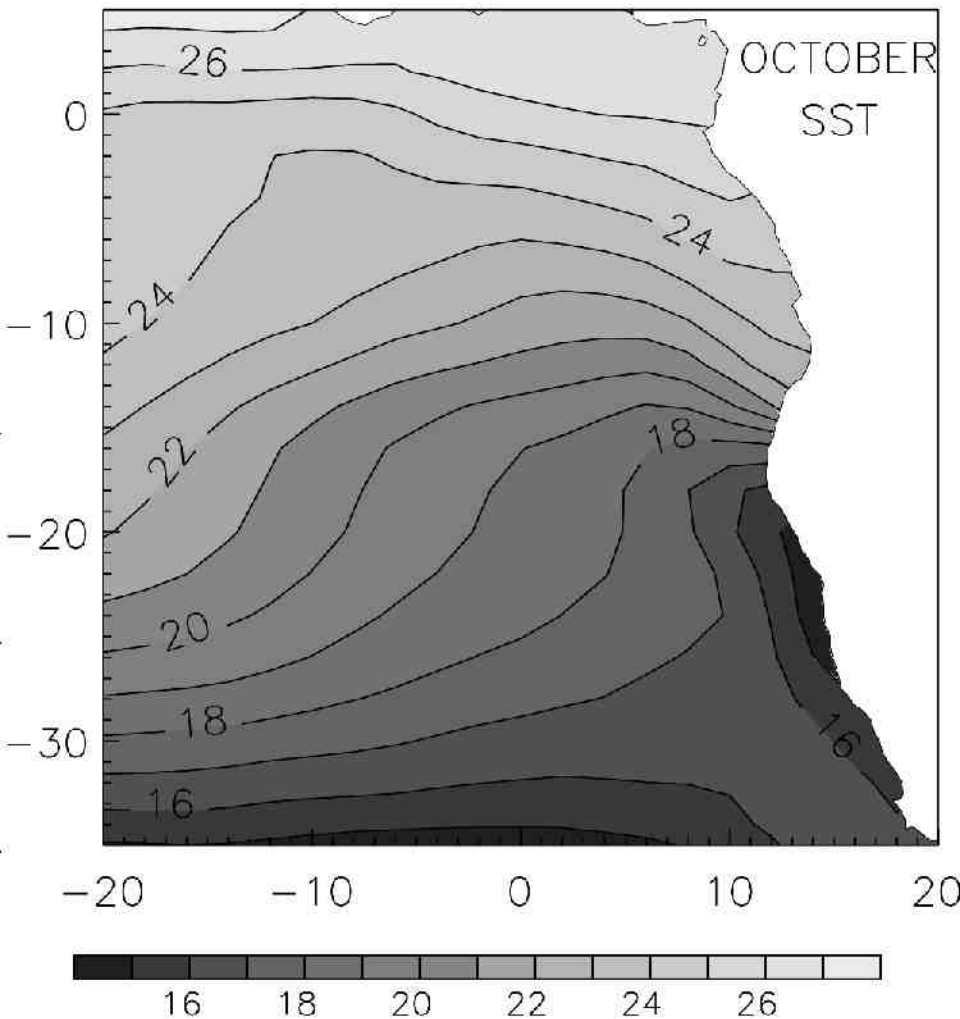


Figure 8. Mean sea-surface temperatures ($^{\circ}$ C) in the southeastern Atlantic (October mean for the period 1948 to 2005).

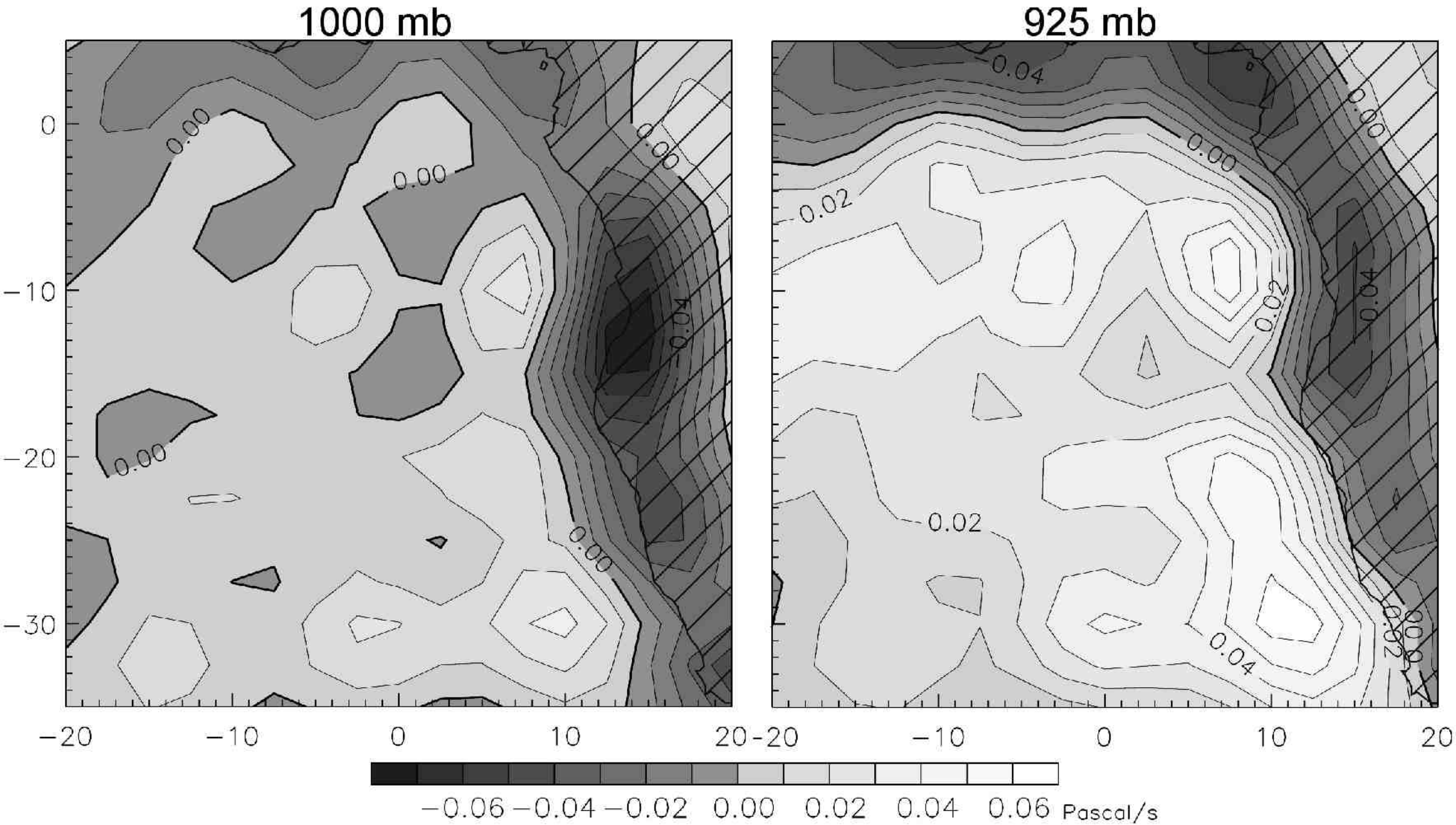


Figure 9. Mean omega (vertical motion, pascals s^{-1}) at 1000 and 925 hPa for October.

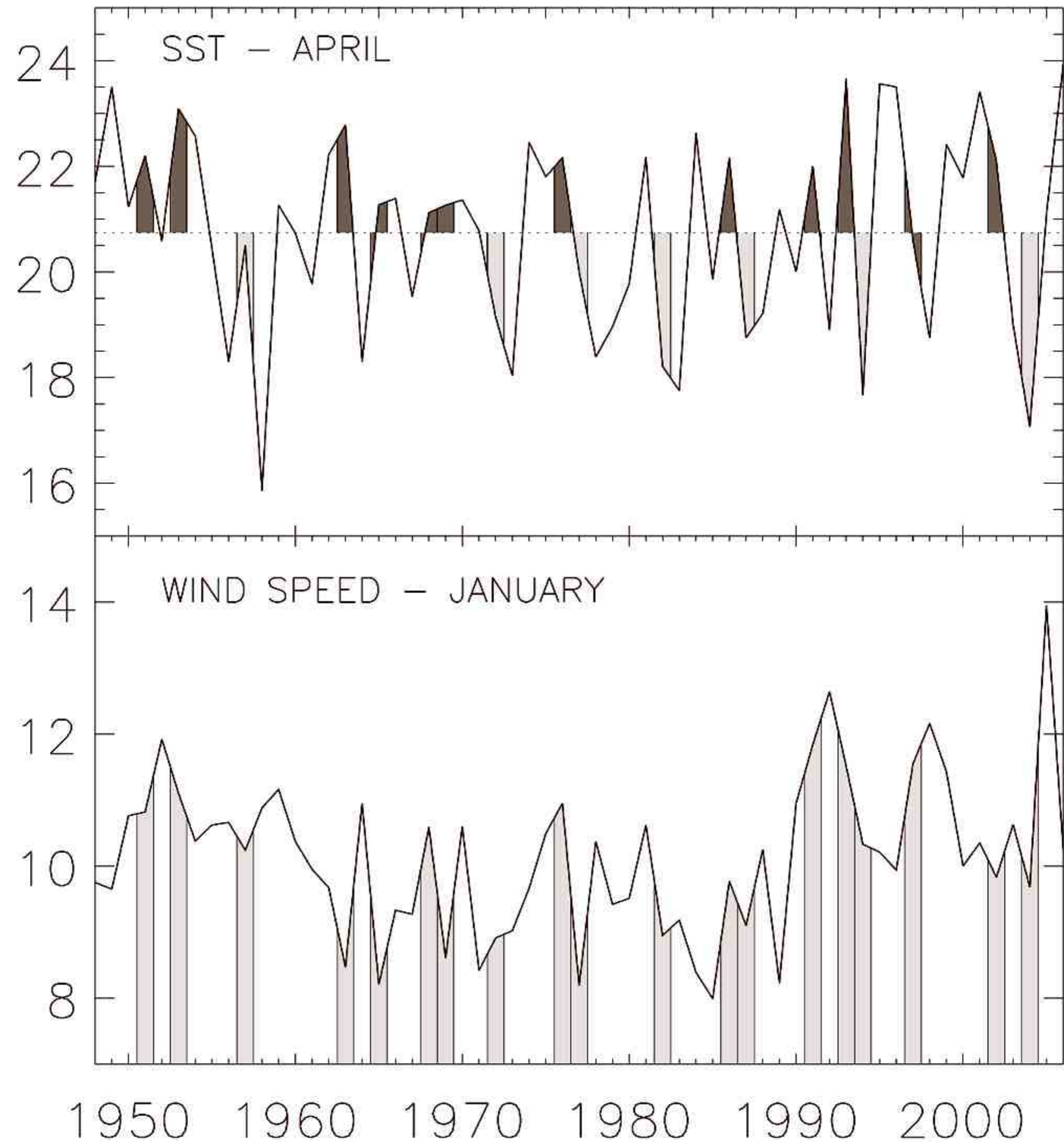


Figure 10a. April SSTs (17° S, 5° E to 15° E) and January wind speeds in the core of the Benguela jet, at 1000 hPa, 1948 to 2005 (from Nicholson 2007). The core speed of the Benguela Jet is defined as the maximum wind speed at 1000 hPa within the box shown in Fig. 7. El Niño years are shaded.

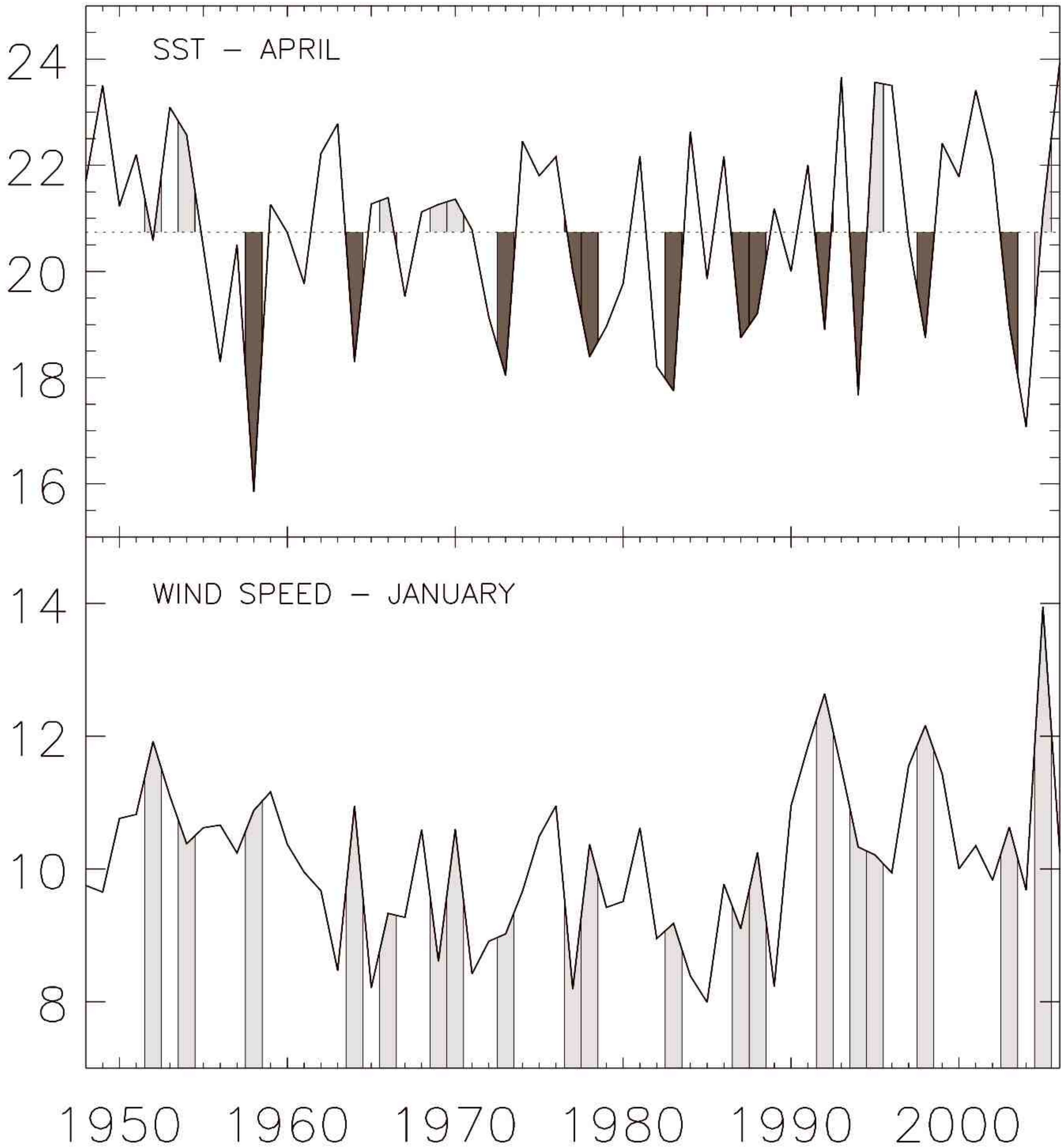


Figure 10b. As in 10 a, but post-el Niño years are shaded.

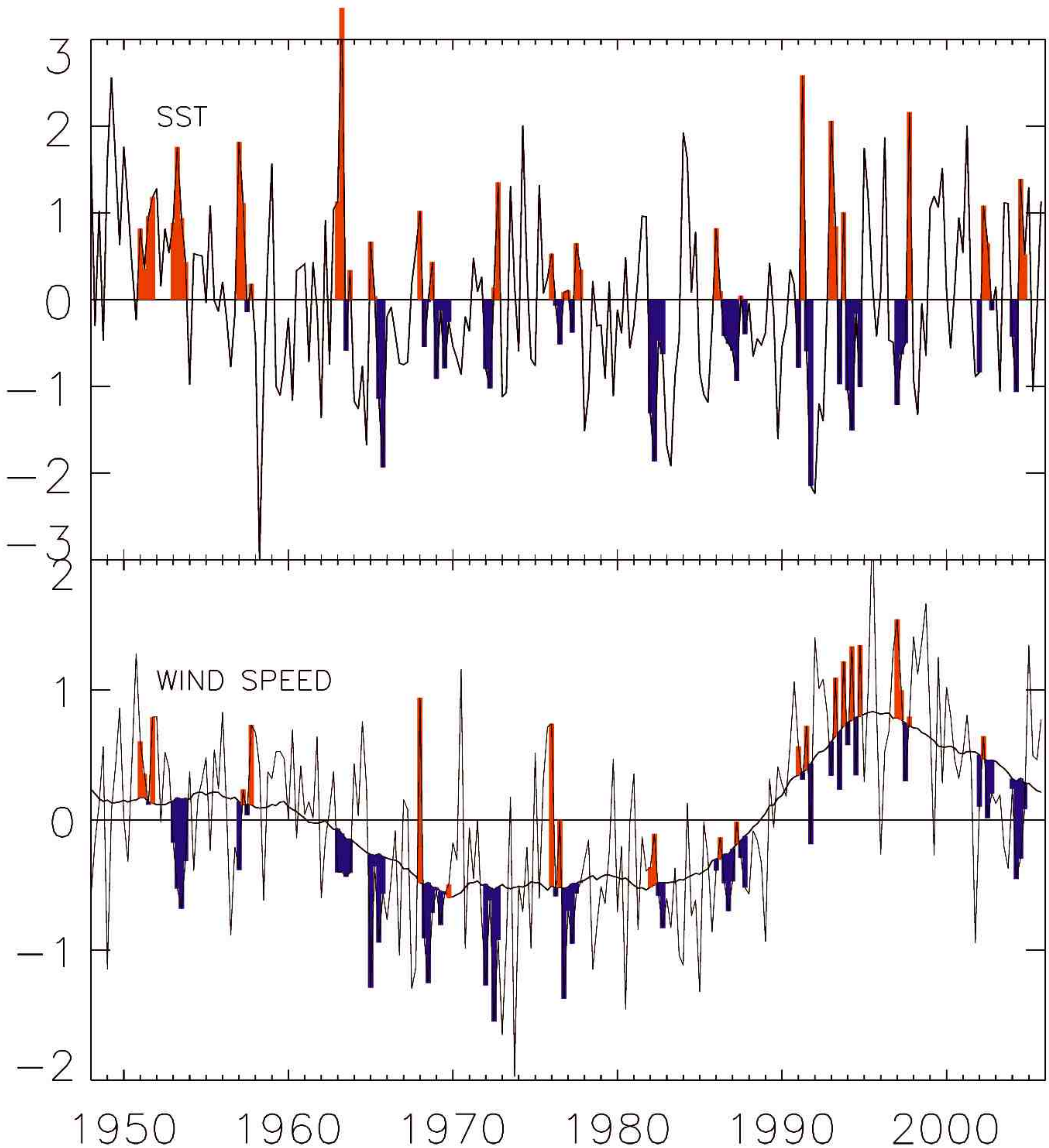


Figure 11. (top) Three-month means of SST anomalies at 17° S (5° E to 15° E), 1948 to 2005 (el Niño years are shaded). (bottom) Core speed of the Benguela Jet, expressed as a three-month departure from the seasonal mean at the location of maximum 1000 hPa winds within the box shown in Fig. 7. Shading expresses departures from a running ten-year mean.

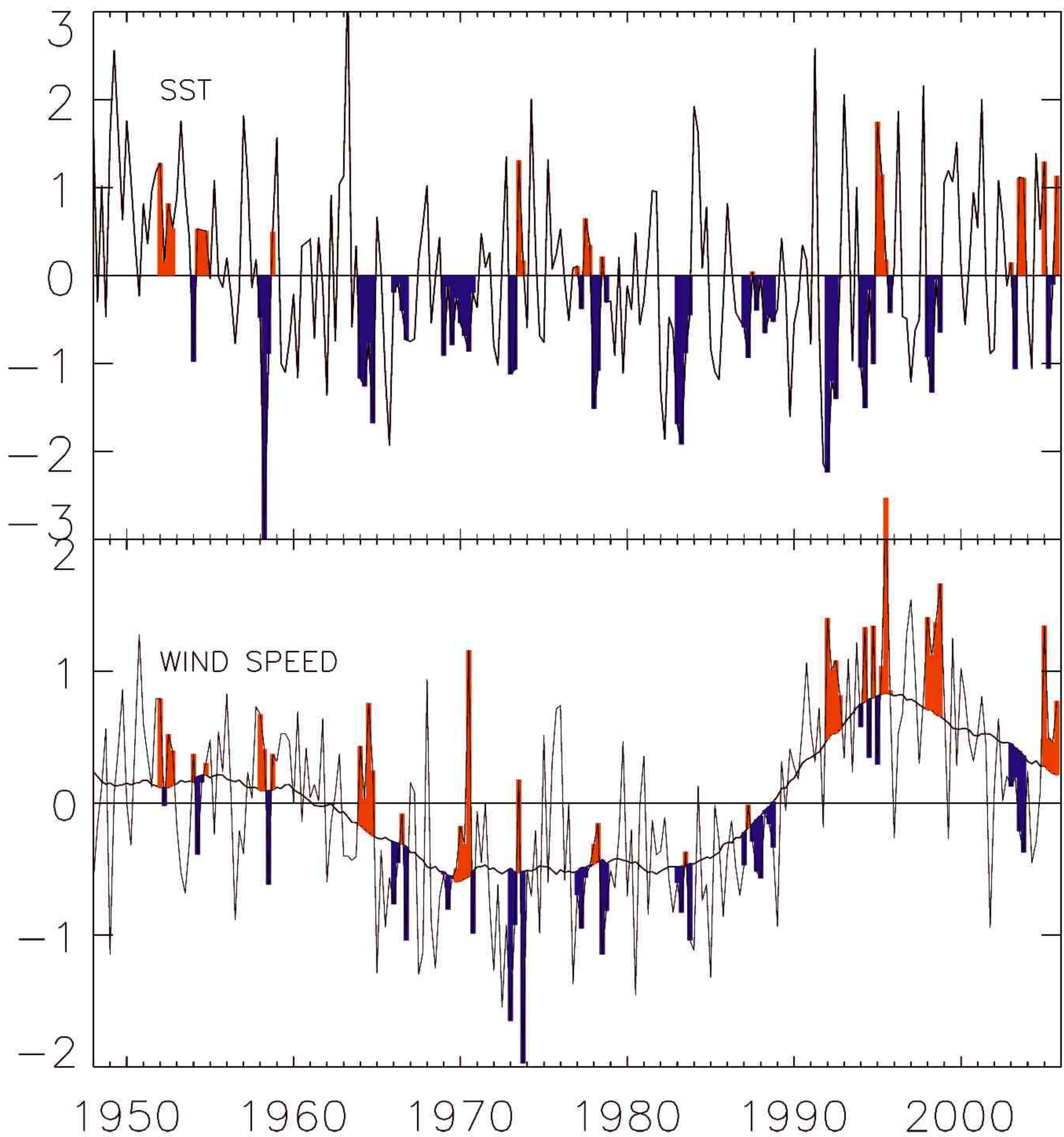


Figure 12. (top) Three-month means of SST anomalies at 17° S (5° E to 15° E), 1948 to 2005 (post el Niño years are shaded). (bottom) Core speed of the Benguela Jet, as in Fig. 11.